MBX-102/JNJ39659100, a Novel Peroxisome Proliferator-Activated Receptor-Ligand with Weak Transactivation Activity Retains Antidiabetic Properties in the Absence of Weight Gain and Edema

Francine M. Gregoire, Fang Zhang, Holly J. Clarke, Thomas A. Gustafson, Dorothy D. Sears, Svetlana Favelyukis, James Lenhard, Dennis Rentzeperis, L. Edward Clemens, Yi Mu, and Brian E. Lavan

Metabolex (F.M.G., H.J.C., L.E.C., Y.M., B.E.L.), Department of Biology, Hayward, Californaia 94545; Lilly Research Laboratories (F.Z.), Indianapolis, Indiana 46285; Pfizer, Inc. (T.A.G.), Groton, Connecticut 06340; Department of Medicine (D.D.S., S.F.), Division of Endocrinology and Metabolism, University of California, San Diego, California 92103; and Johnson & Johnson PRD (J.L., D.R.), Exton, Pennsylvania 19341

MBX-102/JNJ39659100 (MBX-102) is in clinical development as an oral glucose-lowering agent for the treatment of type 2 diabetes. MBX-102 is a nonthiazolidinedione (TZD) selective partial agonist of peroxisome proliferator-activated receptor (PPAR)-γ that is differentiated from the TZDs structurally, mechanistically, preclinically and clinically. In diabetic rodent models, MBX-102 has insulin-sensitizing and glucose-lowering properties comparable to TZDs without dose-dependent increases in body weight. *In vitro*, in contrast with full PPAR-γ agonist treatment, MBX-102 fails to drive human and murine adipocyte differentiation and selectively modulates the expression of a subset of PPAR-γ target genes in mature adipocytes. Moreover, MBX-102 does not inhibit osteoblastogenesis of murine mesenchymal cells. Compared with full PPAR-γ agonists, MBX-102 displays differential interactions with the PPAR-γ ligand binding domain and possesses reduced ability to recruit coactivators. Interestingly, in primary mouse macrophages, MBX-102 displays enhanced antiinflammatory properties compared with other PPAR-γ or α/γ agonists, suggesting that MBX-102 has more potent transrepression activity. In summary, MBX-102 is a selective PPAR-γ modulator with weak transactivation but robust transrepression activity. MBX-102 exhibits full therapeutic activity without the classical PPAR-γ side effects and may represent the next generation insulin sensitizer. **(*Molecular Endocrinology* 23: 975–988, 2009)**

Peroxisome proliferator-activated receptor (PPAR)-γ belongs to the nuclear receptor superfamily of transcription factors and is a member of the NR1C subgroup that includes PPAR-α and PPAR-δ. PPARs are ligand-activated nuclear receptors that display a wide range of biological effects. Although PPAR-γ is most abundantly expressed in adipose tissue and is a known activator of fat cell formation, PPAR-γ also negatively regulates osteoblastogenesis (1) and has recently emerged as a key modulator of inflammatory and immune responses (2). PPAR-γ ligands include a surprisingly diverse array of natural and synthetic molecules among which the thiazolidinediones (TZDs) are the best characterized (3, 4).

PPAR-γ activates transcription in a ligand-dependent manner by binding directly to specific PPAR-response elements in target genes as a heterodimer with the retinoic X receptor. Agonist binding within the PPAR-γ ligand-binding domain (LBD) causes conformational changes leading to the exchange of corepressor for coactivator proteins and a switch from gene repression to activation (5). Synthetic PPAR-γ ligands described as full agonists appear to share a common binding mode, in which the

Abbreviations: ATRA, All-trans-retinoic acid; CBP, CREB-binding protein; ChIP, chromatin immunoprecipitation; DMSO, dimethylsulfoxide; ET-1, endothelin-1; FABP4, fatty acid-binding protein 4; FBS, fetal bovine serum; FCB, fat cell buffer; FRET, fluorescence resonance energy transfer; GyK, glycerol kinase; HRP, horseradish peroxidase; LBD, ligand-binding domain; LPS, lipopolysaccharide; MCP-1, moncyte chemoattractant protein-1; NCoR, nuclear receptor corepressor; PEPCK, phosphoenolpyruvate carboxykinase; PGC1α, PPAR-γ coactivator 1α; PPAR, peroxisome proliferator-activated receptor; siRNA, small interfering RNA; SMRT, silencing mediator for retinoid and thyroid-hormone receptor; SP1, selective partial PPAR-γ agonist 1; SP2, selective partial PPAR-γ agonist 2; SRC1, steroid receptor coactivator 1; TIF2, transcriptional intermediary factor 2; TR, time resolved; TRAP220, thyroid hormone receptor associated protein 220; TZD, thiazolidinedione; WT, wild type; ZDF, Zucker diabetic fatty; ZF, Zucker fatty; ZL, Zucker lean.

ISSN Print 0888-8809 ISSN Online 1944-9917
Printed in U.S.A.

doi: 10.1210/me.2008-0473 Received December 22, 2008. Accepted April 14, 2009.
First Published Online April 30, 2009

acidic head groups interact with three key amino acid residues (H323, H449, and Y473) within the ligand-binding pocket. These interactions configure the C-terminal activation function 2 domain to form a charge clamp in which a conserved glutamate in the activation function 2 helix and a conserved lysine in the LBD grip the LXXLL-containing helical motifs present in most nuclear receptor coactivators (5–7). Interestingly, synthetic ligands that induce partial PPAR-γ transactivation in cell-based assays bind the LBD in a different manner and do not directly interact with the AF-2 helix. These partial agonists exhibit reduced ability to recruit coactivators, diminished adipogenic capacity, and attenuated gene signatures in cultured adipocytes (8–10). Benefits of PPAR-γ activation are demonstrated by the current clinical use of PPAR-γ modulating agents as antidiabetic drugs. Actos (pioglitazone) and Avandia (rosiglitazone), two potent PPAR-γ agonists of the TZD class, induce remarkable insulin sensitization and improved glycemic control in patients with type 2 diabetes (11, 12). However, despite their proven efficacy, these drugs possess a number of deleterious class-related side effects, including significant weight gain, peripheral edema, increased risks of congestive heart failure, and increased rate of bone fracture (13–16). Such major safety concerns have not only restrained the clinical use of these drugs but have also led to the failed development of many PPAR agonists (4, 16).

In addition to the well-studied effects of PPAR-γ on adipocyte differentiation and insulin sensitization, there is a growing body of evidence demonstrating that PPAR-γ also plays a key role in the regulation of immunity and inflammation (17–19). In this respect, the antiinflammatory properties of PPAR-γ agonists have recently emerged as putative effectors of their antidiabetic activities. Disruption of PPAR-γ in macrophages leads to insulin resistance and glucose intolerance and to a decreased response to TZDs treatment (17, 20, 21). Although the detailed molecular mechanisms responsible for this effect are not fully understood, PPAR-γ is likely to play a role by negatively regulating the production of macrophage-derived inflammatory mediators known to promote insulin resistance (18). Studies indicate that PPAR-γ inhibits inflammatory gene expression in activated macrophages by a nuclear receptor corepressor (NCoR)/sumoylation-dependent pathway (22). Interestingly, it was suggested that ligand-induced allosteric changes in PPAR-γ that regulate this transrepression pathway are distinct from those that mediate interaction with conventional coactivators (17). Thus, it may be possible to develop optimized, safer PPAR-γ ligands that would preferentially transrepress inflammatory genes rather than transactivate detrimental metabolic genes, thereby retaining their antidiabetic activity in the absence of side effects.

During the last decade, a major investment was made by the pharmaceutical industry to develop safer PPAR agonists. Although this effort led to the description of several unique selective partial PPAR-γ agonists (4, 16, 23–27), most of these compounds have not been characterized *in vivo*, making it difficult to determine whether their safety margin has been improved when compared with the currently marketed PPAR-γ agonists.

Halofenate is a racemic mixture of (−)- and (+)-[2-acetoaminoethyl (4-chlorophenyl) (3-trifluoromethylphenoxy) acetate] that was clinically tested in the 1970s as a hypolipidemic and hypouricemic agent (28). In addition to triglyceride and uric acid lowering, significant improvements in glucose tolerance and decreased fasting plasma glucose were observed in type 2 diabetics (29, 30). The insulin sensitization properties of halofenate involve PPAR-γ activation because halofenate was recently identified as a non-TZD, selective partial PPAR-γ agonist (31). Although the antidiabetic activities of halofenate were comparable to those of rosiglitazone, halofenate was clearly differentiated from the full agonist by its inability to promote adipogenesis *in vitro* or weight gain *in vivo* (31).

We selected MBX-102, the (−) enantiomer of halofenate for further clinical development, and it is currently in phase II clinical development as an oral glucose-lowering agent for the treatment of type 2 diabetes. In this report, we demonstrate that MBX-102 is a PPAR agonist selective for the PPAR-γ receptor. Like halofenate, MBX-102 is a weak transactivator of PPAR-γ and possesses equivalent antidiabetic properties without displaying the classical PPAR-γ-linked side effects observed with full agonists. Importantly, we show that MBX-102 potently transrepresses inflammatory genes. These findings suggest that MBX-102 preferentially activates PPAR-γ transrepression rather than coactivator recruitment and transactivation and potentially explain its antidiabetic efficacy in the absence of side effects.

Results

MBX-102 acid is a selective partial PPAR-γ agonist that is distinct from rosiglitazone

MBX-102 (Fig. 1A) is the (−) enantiomer of halofenate, a drug previously described as a partial PPAR-γ agonist (31). MBX-102 is a pro-drug ester (Fig. 1A), that is rapidly and completely modified *in vivo* by nonspecific serum esterases to the mature free acid form MBX-102 acid (Fig. 1B), which is the circulating form of the drug. For these reasons, MBX-102 was used for *in vivo* studies whereas the acid form was used for all *in vitro* studies.

To investigate whether MBX-102 acid behaves as a PPAR-γ agonist, its ability to bind and activate PPAR-γ *in vitro* was determined. As shown in Fig. 1C, MBX-102 acid completely displaced a fluorescent PPAR-γ ligand from the ligand-binding domain (LBD) of human PPAR-γ in a dose-dependent manner. In this assay, MBX-102 acid and rosiglitazone displayed IC_{50}s of approximately 35 and about 0.1 μM, respectively. Dose-dependent activation of human GAL4-PPAR-γ was also observed in response to MBX-102 acid and rosiglitazone, with EC_{50}s of about 12 μM for MBX-102 acid and approximately 1 μM for rosiglitazone (Fig. 1D). The maximal transactivation activity of MBX-102 acid was about 10% of that observed with rosiglitazone (Fig. 1D), suggesting MBX-102 acid functions as a partial PPAR-γ agonist in this context. This weak degree of transactivation of PPAR-γ was similar in three different cell lines (HEK, CHO, and CV1 cells; data not shown). MBX-102 did not trans-

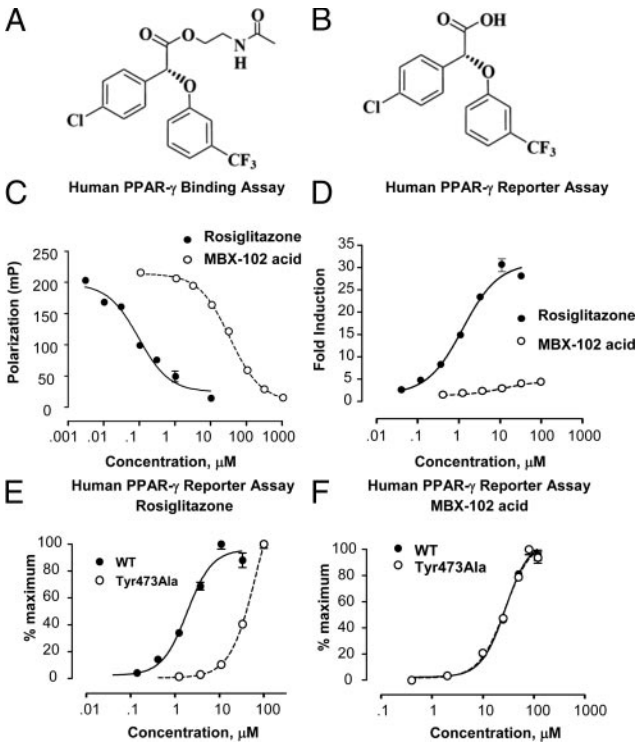

FIG. 1. Chemical structures of MBX-102: prodrug ester (panel A) and mature free acid form (panel B). C, Competitive binding assay. D, Reporter assay using a GAL4-PPAR-γ LBD chimera. E and F, Determination of the requirement for LBD Tyr 473 for the activation of PPAR-γ by rosiglitazone (E) or MBX-102 acid (F) as assessed by comparing WT PPAR-γ to Tyr473Ala PPAR-γ. Values are plotted as mean ± SEM and are representative of at least three independent experiments. mP, Milli-Polarization level.

activate human GAL4-PPAR-α or -δ (supplemental Fig. 1 published as supplemental data on The Endocrine Society's Journals Online web site at http://mend.endojournals.org), indicating that MBX-102 acid is highly selective for human PPAR-γ. A very similar PPAR-activation profile of MBX-102 acid was observed for mouse and rat orthologs, including the absolute selectivity for PPAR-γ, the degree of partial agonism, and EC_{50}s for PPAR-γ activation (supplemental Fig. 1 and supplemental Table 1). MBX-102 acid also had the ability to antagonize rosiglitazone-dependent PPAR-γ activation (supplemental Fig. 2), suggesting that the site of binding for MBX-102 acid overlaps with that of rosiglitazone and supporting the characterization of MBX-102 acid as a partial agonist. Interaction with Tyr473 in helix 12 of the LBD of PPAR-γ is required for the functional activity of full agonists, and mutation of Tyr473 to alanine (Y473A) abolishes the ability of full agonists to activate PPAR-γ (24, 32). The requirement of Tyr473 for the activity of MBX-102 acid was assessed using GAL4-human PPAR-γ LBD containing the Y473A mutation. As expected, the Y473A mutation significantly compromised the potency of rosiglitazone and right shifted its transactivation curve with a 36-fold increase in EC_{50} (WT, ~1.9 μM; Y473A, ~69 μM) (Fig. 1E). In contrast, the Y473A mutation had no effect on the ability of MBX-102 acid to activate PPAR-γ (EC_{50}: WT, ~28 μM; Y473A ~27 μM) (Fig. 1F). These data indicate that MBX-102 binds to the PPAR-γ LBD in a manner that is distinct from but overlapping with rosiglitazone. These results were not unexpected given that partial and full PPAR-γ agonists bind in the same ligand-binding pocket but may bind in a different manner (10).

MBX-102 acid increases insulin sensitivity of 3T3-L1 adipocytes, and the insulin sensitization effect is PPAR-γ dependent

PPAR-γ plays a central role in glucose metabolism. TZDs sensitize adipocytes to insulin as shown by increased glucose uptake at submaximal insulin concentrations. The ability of MBX-102 acid to modulate the insulin sensitivity of 3T3-L1 adipocytes was investigated. The PPAR-γ dependency of the insulin sensitization was simultaneously assessed by using small interfering RNA (siRNA)-mediated PPAR-γ gene silencing.

Differentiated 3T3-L1 adipocytes were treated with dimethylsulfoxide (DMSO), rosiglitazone, or MBX-102 acid in the presence of a submaximal concentration of insulin (0.05 nM), or with endothelin-1 (ET-1, a PPAR-γ-independent stimulator of glucose transport) alone.

In PPAR-γ-containing adipocytes, both insulin and ET-1 increased glucose transport. Insulin-stimulated glucose transport was further enhanced by treatment with either rosiglitazone or MBX-102 acid (Fig. 2A). In PPAR-γ-deficient adipocytes, the enhancement of insulin-stimulated glucose uptake by both PPAR-γ ligands was abolished, confirming the PPAR-γ dependence of the insulin sensitization effect. PPAR-γ silencing was confirmed both at the protein (Fig. 2B) and mRNA (Fig. 2C) levels and was found to be greater than 90%. Near identical results were obtained using a siRNA targeting a different sequence in PPAR-γ (supplemental Fig. 3). ET-1-stimulated glucose uptake was unaffected by PPAR-γ silencing, confirming that the glucose transport system in the PPAR-γ-silenced adipocytes remained intact (Fig. 2A).

MBX-102 displays robust antidiabetic and insulin-sensitizing properties in rodent diabetic models

Antidiabetic properties including glucose lowering in preclinical models is a hallmark of full PPAR-γ agonists and has also been reported for partial agonists (27). The antidiabetic properties of MBX-102 were evaluated by assessing its glucose-lowering activity in several rodent models of type 2 diabetes, including *ob/ob*, *db/db* mice, and Zucker fatty diabetic (ZDF) rats. In all models tested, short-term treatment with MBX-102 led to robust, significant glucose lowering (Table 1).

The ability of MBX-102 to cause insulin sensitization was also examined *in vivo*. ZDF rats were treated for 4–7 d with either vehicle or MBX-102 (100 mg/kg) after which their insulin sensitivity was determined using a hyperinsulinemic-euglycemic clamp. A significant reduction in plasma insulin was observed after MBX-102 treatment (Table 2). When compared with the control group, MBX-102-treated rats showed significant increases in the glucose infusion rate (Fig. 3A) and in the rate of glucose disposal (Rd Clamp values) (Fig. 3B), suggesting that MBX-102 increases insulin sensitivity and glucose utilization in peripheral tissues. In addition, compared with the control rats, MBX-102-treated rats also showed significantly decreased hepatic glucose output in the clamped state (Fig. 3C), suggesting that MBX-102 may also positively affect liver insulin sensitivity in ZDF rats.

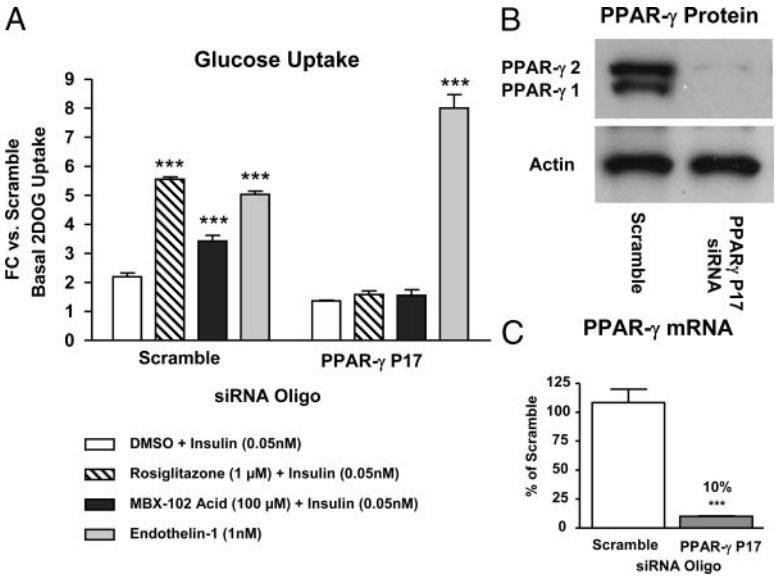

FIG. 2. MBX-102 acid enhances insulin sensitivity *in vitro* in 3T3-L1 adipocytes. Rosiglitazone and MBX-102 acid enhanced glucose uptake activity at submaximal concentration of insulin (0.05 nM) in 3T3-L1 adipocytes (A, Scramble). Silencing of PPAR-γ with P17 siRNA duplexes, as assessed at the protein (B) and message levels (C), fully abolished enhancement by both PPAR-γ agonists (A, PPAR-γ P17). In contrast, enhancement of basal glucose transport by ET-1 was not abolished in PPAR-γ-deficient adipocytes (A, PPAR-γ P17), indicating the cells were able to properly respond to non-PPAR-γ stimuli. Values represent mean ± SEM (n = 4; **, $P < 0.001$ *vs.* DMSO-treated adipocytes, two-way ANOVA and Bonferroni multiple comparison test). FC, Fold change.

Long-term treatment with MBX-102 led to comparable efficacy compared with rosiglitazone while lacking the typical PPAR-γ side effects

Full PPAR-γ agonists cause unwanted side effects such as body weight gain, edema, and increased risk of congestive heart failure (4). To examine MBX-102 therapeutic efficacy and safety profile, a long-term study using the Zucker Fatty (ZF) insulin-resistant rat model was performed (Fig. 4). Multiple doses of MBX-102 and rosiglitazone were administered for 50 d to male ZF rats. Doses of 3, 10, 30, 60, and 100 mg/kg of MBX-102 and 0.3, 1, 3, 10, and 30 mg/kg of rosiglitazone were used. As shown in Fig. 4A, treatment with both compounds led to a dramatic decrease in plasma insulin levels. Maximal insulin lowering was detected with 10 mg/kg of rosiglitazone and 60 mg/kg of MBX-102. Both drug treatments also resulted in a dose-dependent, significant decrease in the insulin resistance index (Fig. 4B), which was assessed after 43 d of treatment by performing an oral glucose tolerance test (supplemental Fig. 4). The magnitude of the decrease in insulin resistance was comparable between the two compounds at high doses (10 and 30 mg/kg of rosiglitazone; 60 and 100 mg/kg of MBX-102; Fig. 4B). A pronounced, dose-dependent lowering of triglyceride was observed with all doses of both compounds (Fig. 4C). Moreover, treatment with 30 mg/kg of either MBX-102 or rosiglitazone led to maximal increases in plasma adiponectin levels (Fig. 4D). These results demonstrate that MBX-102 has physiological efficacy that is equivalent to the full agonist rosiglitazone.

In contrast, MBX-102 and rosiglitazone displayed very different side effect profiles (Fig. 4, E–H). Body weight was elevated after rosiglitazone treatment but not by MBX-102 (Fig. 4E). Rosiglitazone caused a gradual, dose-dependent, significant increase in cumulative body weight gain at doses as low as 1 mg/kg whereas no significant increase in body weight gain was observed with MBX-102 at any dose (supplemental Fig. 5A). Differential modulation of food intake was also recorded between both drugs (supplemental Fig. 5B). Heart weight was unaffected by MBX-102 treatment, but a significant increase was observed at the highest dose of rosiglitazone tested (30 mg/kg; Fig. 4F). Increased heart weight has been observed in preclinical studies with other PPAR-γ agonists, is related to increases in plasma volume, and may be predictive of edema (33). Rosiglitazone markedly increased the mass of the epididymal white adipose (EWAT, Fig. 4G) and of the intrascapular brown adipose (IBAT, Fig. 4H) in a dose-dependent manner, whereas marginal increases were detected only with the highest dose of MBX-102 (Fig. 4, G and H). These observations confirm that, at equivalently efficacious doses, MBX-102 displays a more desirable side effect profile compared with rosiglitazone.

MBX-102 acid is less adipogenic than rosiglitazone and differentially regulates PPAR-γ-responsive genes in human and murine adipocytes

To understand why MBX-102 does not induce weight and adipose tissue gain in preclinical species, we evaluated the ability of MBX-102 acid to drive adipogenesis in human and rodent cell-based systems. As shown in Fig. 5, rosiglitazone induced significant adipogenesis in human primary preadipocytes as indicated by the pronounced increase in Oil-red-O staining (Fig. 5A) and triglyceride content (Fig. 5B). In contrast, MBX-102 acid displayed significantly reduced ability to drive human adipocyte differentiation (Fig. 5, A and 5B). Similarly, MBX-102

TABLE 1. MBX-102 lowers fasting plasma glucose levels in diabetic rodent models

Animal model	Treatment duration (days)	Mean fasting plasma glucose ± SEM (mg/dl)		
		Vehicle	Rosiglitazone	MBX-102
ob/ob	12	426.1 ± 34.7 (n = 12)	224.5 ± 17.0[a] (n = 12)	190.4 ± 29.3[a] (n = 12)
db/db	9	409.9 ± 40.1 (n = 12)	177.9 ± 8.4[a] (n = 12)	221.9 ± 9.8[a] (n = 8)
ZDF	11	397.0 ± 57.5 (n = 6)	144.7 ± 10.9[a] (n = 6)	184.8 ± 17.2[b] (n = 6)

ob/ob Mice were orally dosed daily with vehicle (5 ml/kg), rosiglitazone (10 mg/kg), or MBX-102 (125 mg/kg). *db/db* Mice were orally dosed daily with vehicle (5 ml/kg), rosiglitazone (10 mg/kg), or MBX-102 (250 mg/kg). Male ZDF rats were orally dosed daily with vehicle (5 ml/kg), rosiglitazone (4 mg/kg), or MBX-102 (100 mg/kg).

[a] $P < 0.001$ *vs.* vehicle group; [b] $P < 0.01$; one-way ANOVA and Tukey's multiple comparison test).

TABLE 2. General characteristics of the experimental ZDF rats used for the clamp study

	Vehicle	MBX-102 (100 mg/kg)
Posttreatment body weight (g)	353.4 ± 5.4	351.2 ± 6.0[a]
Basal glucose concentration (mg/dl)	183.1 ± 20.5	134.2 ± 8.1[a]
Clamped glucose concentration (mg/dl)	152.2 ± 2.2	159.1 ± 1.1[a]
Basal insulin concentration (ng/ml)	11.8 ± 1.1	4.6 ± 1.1[b]

Values represent mean ± SEM (n = 7 for vehicle-treated group and n = 6 for MBX-102-treated group. [a] $P > 0.05$; [b] $P < 0.001$ *vs.* vehicle-treated, unpaired two-tailed *t* test).

acid also displayed markedly decreased ability to stimulate differentiation of murine 3T3-L1 preadipocytes (supplemental Fig. 6).

When compared with rosiglitazone, MBX-102 acid was also found to differentially regulate adipogenic and lipogenic genes in human differentiated primary adipocytes (Fig. 5C). As anticipated, rosiglitazone significantly induced the expression of phosphoenolpyruvate carboxykinase (PEPCK), fatty acid-binding protein 4 (FABP4), and CD36, whereas MBX-102 acid showed attenuated induction. In 3T3-L1 adipocytes, MBX-102 acid modulated some, but not all, of the PPAR-γ responsive genes evaluated. Specifically, MBX-102 acid and rosiglitazone similarly decreased the mRNA levels of 11β-hydroxysteroid dehydrogenase type 1 (HSD11B1) and increased the mRNA levels of pyruvate dehydrogenase kinase 4 and ANGPTL4 (Fig. 5D).

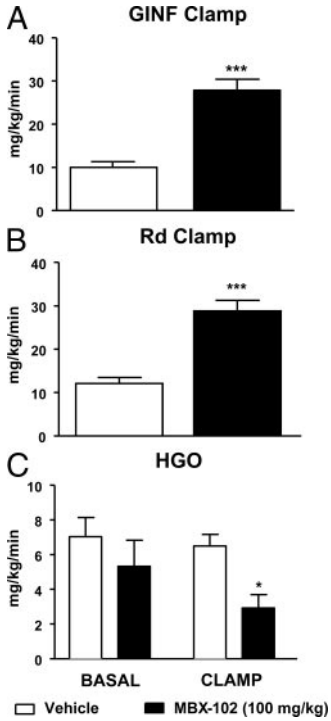

FIG. 3. MBX-102 displays insulin sensitization activity *in vivo*. Glucose disposal was evaluated in ZDF rats using hyperinsulinemic-euglycemic clamp. The clamped glucose infusion rate (GINF) (A), rate of glucose disposal (R_d) (B), and hepatic glucose output (HGO) (C) rate were measured at steady state. Values are mean ± SEM, n = 7 for vehicle-treated and n = 6 for MBX-102-treated groups (*, $P < 0.05$ *vs.* vehicle group, two-way ANOVA and Bonferroni posttests; ***, $P < 0.001$ *vs.* vehicle group, unpaired two-tailed *t* test).

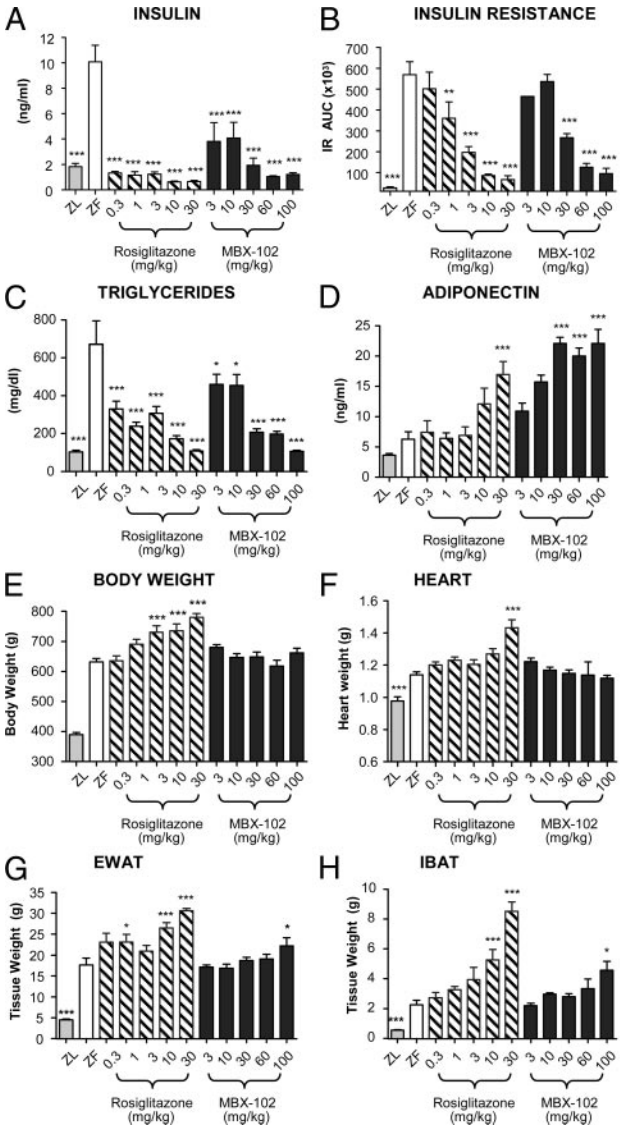

FIG. 4. ZF rat study: long-term efficacy (A–D) and side effects (E–H). For all groups, the insulin resistance index (B) was assessed after 43 d of drug treatment whereas all other parameters (A, C–H) were assessed after 50 d of drug treatment. ZL, Vehicle-treated ZL rats; ZF, vehicle-treated ZF rats; EWAT, epididymal white adipose tissue, IBAT, intrascapular Brown adipose tissue. Values are mean ± SEM (n = 6–8/group; *, $P < 0.05$; **, $P < 0.01$; ***, $P < 0.001$ *vs.* ZF vehicle, one-way ANOVA and Dunnett's multiple comparison test).

As observed in human adipocytes, rosiglitazone induced the expression of key lipogenic genes including glycerol kinase (GyK), PEPCK, FABP4 and CD36, whereas MBX-102 acid showed little (GyK, PEPCK) to no induction (FABP4, CD36) of these same genes (Fig. 5E).

MBX-102 acid displays differential recruitment of coactivators compared with rosiglitazone

Ligand-dependent nuclear hormone receptor activation regulates gene expression through the dissociation of corepressors and subsequent recruitment of coactivators (34). The differential binding of MBX-102 acid to the PPAR-γ LBD may lead to an alteration in the ability to dissociate corepressors and/or to recruit coactivators, possibly explaining the differential gene regulation observed in mature adipocytes treated with MBX-102 acid

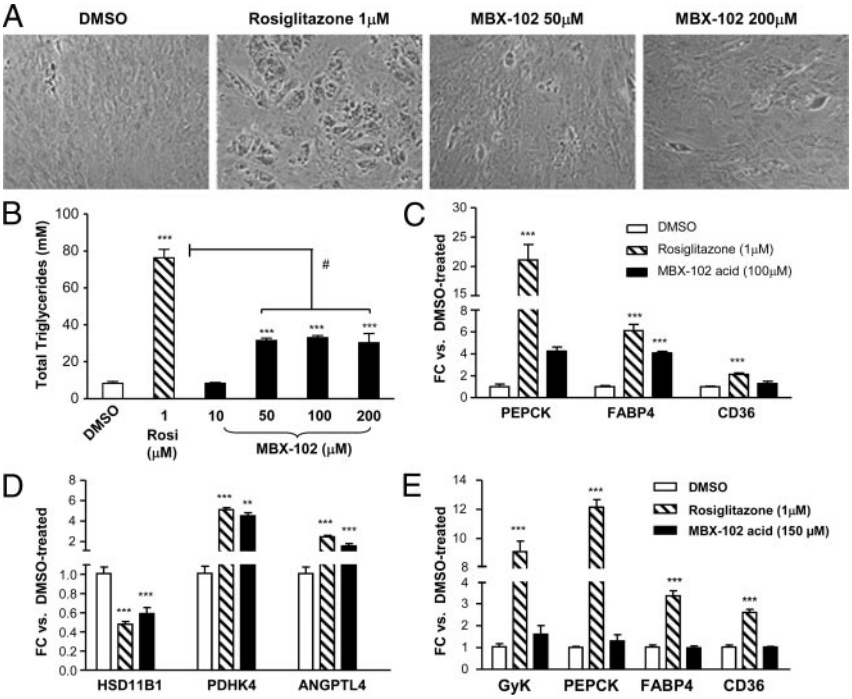

FIG. 5. MBX-102 acid induced less human preadipocyte differentiation than the full PPAR-γ agonist rosiglitazone as assessed by Oil-red-O staining (A) and triglyceride measurements (B). MBX-102 acid also selectively modulated PPAR-γ-responsive genes in differentiated human adipocytes (C). In differentiated 3T3-L1 adipocytes, MBX-102 acid modulated some PPAR-γ-responsive genes similarly (D) and some differentially (E) compared with rosiglitazone. Values represent mean ± SEM and are representative of at least two to three independent experiments (***, $P < 0.001$; one-way ANOVA and Tukey's multiple comparison test). FC, Fold change.

and rosiglitazone. We compared the ability of MBX-102 acid and rosiglitazone to modulate the interaction of corepressors and coactivators with PPAR-γ using a time resolved (TR)-fluorescence resonance energy transfer (FRET) assay. MBX-102 acid was able to efficiently displace the corepressors NCoR and silencing mediator for retinoid and thyroid-hormone receptors (SMRT) in a dose-dependent manner and to a similar degree as rosiglitazone (Fig. 6A). In contrast, MBX-102 acid displayed a greatly reduced ability to recruit coactivators compared with rosiglitazone. The relative magnitude of thyroid hormone receptor associated protein 220 (TRAP220), CREB-binding protein (CBP), or transcriptional intermediary factor 2 (TIF2) recruitment by MBX-102 acid was similar to the degree of transactivation observed in the reporter assays (~11 to 16% of rosiglitazone) whereas slightly better recruitment (~25 to 28% of rosiglitazone) was seen for steroid receptor coactivator 1 (SRC1) and PPAR-γ coactivator 1α (PGC1α) (Fig. 6A).

To examine further the differences in effects of MBX-102 acid and rosiglitazone on PPAR-γ coregulator interactions in a physiologically relevant context, chromatin immunoprecipitation (ChIP) studies were performed using differentiated 3T3-L1 adipocytes. Coregulator association with the promoters of the glycerol kinase GyK and (PEPCK) genes, (two PPAR-γ target genes differentially regulated by MBX-102 acid and rosiglitazone) were assessed. As shown in Fig. 6B, MBX-102 acid significantly decreased the association of the corepressors NCoR and SMRT with both the GyK and PEPCK promoters. Similar findings were observed for rosiglitazone. In contrast, MBX-102 acid was unable to increase the recruitment of coactivators (p300, CBP, and TRAP220) to either promoter whereas robust recruitment of coactivators was observed after treatment with rosiglitazone (Fig. 6B).

Effect of MBX-102 acid on osteoblast/adipocyte differentiation pathways in mesenchymal cells

Osteoblasts and adipocytes are derived from a common cell lineage of progenitor cells present in the bone marrow. Terminal differentiation of these progenitor cells to either osteoblasts or adipocytes depends on the temporal expression of transcription factors and external effectors. Full PPAR-γ agonists promote adipogenesis and reciprocally inhibit osteoblastogenesis. The murine mesenchymal cell line C3H10 T1/2 was used to address the effect of MBX-102 on osteoblast and adipocyte differentiation markers. As shown in Fig. 7A, rosiglitazone treatment of C3H10 T1/2 cells inhibited retinoic-acid [all-*trans*-retinoic acid ATRA)]-stimulated alkaline phosphatase expression, an early marker of bone cell phenotype, whereas treatment with MBX-102 acid did not inhibit the expression of this bone cell marker. Moreover, a high dose of MBX-102 acid was able to partly antagonize the rosiglitazone effect. In addition, rosiglitazone treatment markedly increased triglyceride accumulation in these cells, whereas MBX-102 acid treatment had no effect (Fig. 7B). In this system, MBX-102 acid was also able to fully antagonize the adipogenic capacity of rosiglitazone (Fig. 7B).

MBX-102 displays potent antiinflammatory properties

TZDs have beneficial antiinflammatory effects, and the ability of the PPAR-γ agonist rosiglitazone to repress inflammatory responses in macrophages has recently been demonstrated (for review, see Ref. 2). The antiinflammatory properties of MBX-102 acid were investigated using mouse primary peritoneal macrophages. Before lipopolysaccharide (LPS) treatment, mouse macrophages were treated with either rosiglitazone or MBX-102 acid. Changes in secreted cytokines were evaluated 24 h after LPS treatment. As shown in Fig. 8A, MBX-102 acid decreased the levels of LPS-stimulated proinflammatory cytokines to a greater [moncyte chemoattractant protein-1 (MCP-1), IL-1β, and IL-6] or slightly less (IL-12p40) extent than rosiglitazone. Similar changes were observed at the gene expression level (supplemental Fig. 7). To assess whether the MBX-102 antiinflammatory effects are PPAR-γ dependent, PPAR-γ deficient [knock-out (KO)] primary mouse macrophages were used. As shown in Fig. 8B, PPAR-γ protein levels were dramatically reduced. In these cells, MBX-102 was unable to repress MCP-1, indicating this effect was mediated through PPAR-γ. Similar results were obtained for IL-12p40. In contrast, upon MBX-102 treatment repression of IL-6 was observed both in wild-type (WT) and KO macrophages, suggesting the suppression of IL-6 secretion in

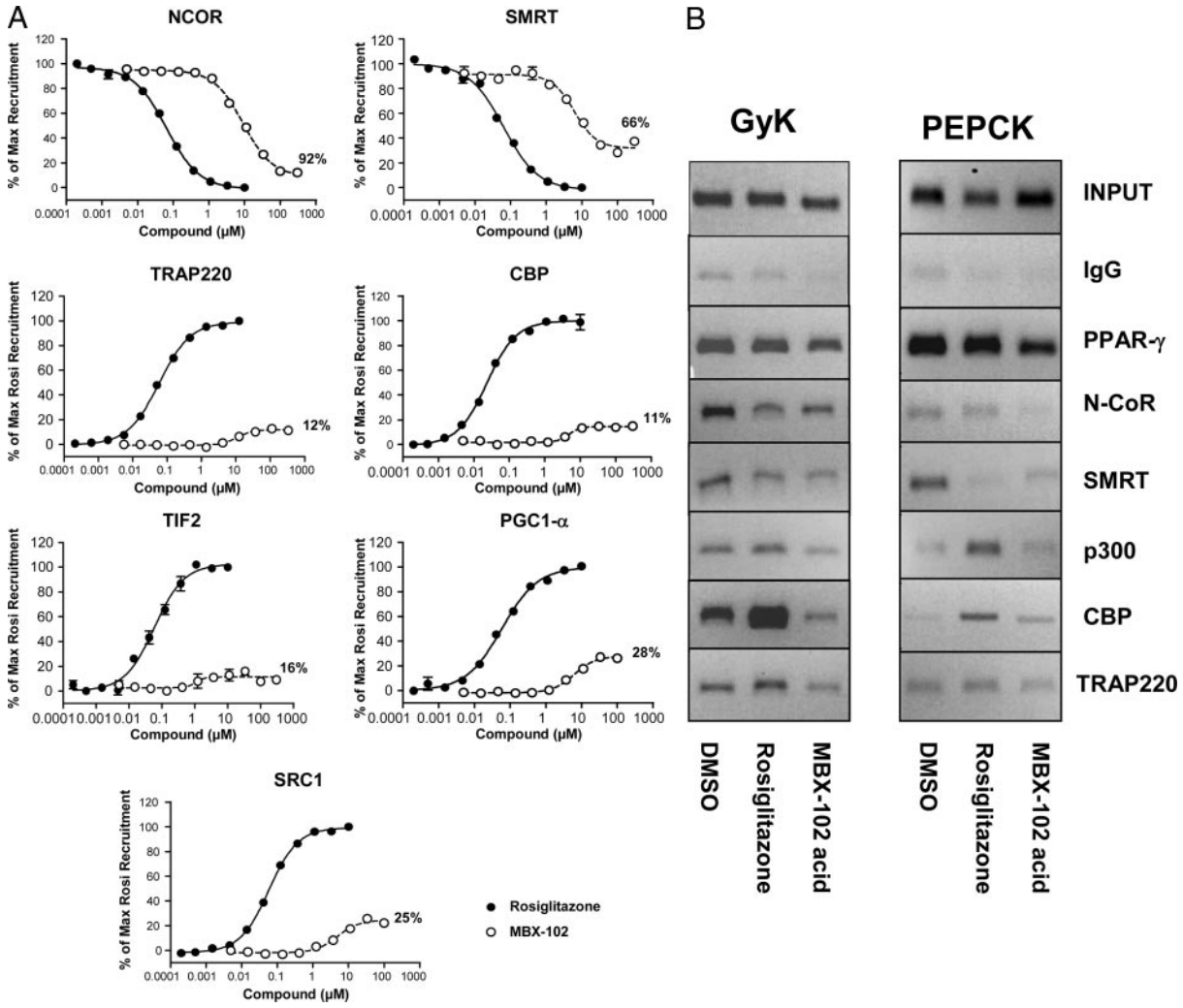

FIG. 6. A, TR-FRET assay was used to examine corepressor peptide displacement from or coactivator recruitment to human PPAR-γ LBD in response to rosiglitazone or MBX-102 acid. Coactivator data are expressed as a percentage of the maximum rosiglitazone response. Corepressor data are expressed as a percentage of the maximum recruitment in the absence of ligand. Two to five independent experiments were performed and representative graphs are shown. B, ChIP analysis of coregulator binding to GyK and PEPCK promoters in 3T3-L1 adipocytes treated with DMSO, rosiglitazone (1 μM), or MBX-102 acid (150 μM). The coregulators assessed included NCoR, SMRT, p300, CBP, and TRAP220. Figures are representative of at least two independent experiments.

these cells is PPAR-γ independent. Interestingly, rosiglitazone retained some ability to transrepress these cytokines in the KO cells. MBX-102 also displayed impressive antiinflammatory properties *in vivo*. Decreased macrophage content and MCP-1 gene expression were found in epididymal adipose tissue derived from both *db/db* mice (data not shown) and ZF rats (supplemental Fig. 8) chronically treated with MBX-102.

MBX-102 displays a unique transactivation/transrepression profile compared with glitazones, glitazars, or other selective partial PPAR-γ agonists

Although MBX-102 acid is a weak transactivator of PPAR-γ, it is a potent transrepressor of proinflammatory genes *in vitro* and *in vivo*. Based on the role of macrophage PPAR-γ and transrepression in the insulin-sensitizing efficacy of PPAR-γ agonists, we compared the transrepression profile of several selective γ [MBX-102, selective partial PPAR-γ agonist 1 (SP1), selective partial PPAR-γ agonist 2 (SP2), troglitazone, rosiglitazone, and pioglitazone] or dual α/γ (muraglitazar and tesaglitazar) PPAR agonists. Compounds were initially selected based on their potential for transactivating FABP4 in 3T3-L1 preadipocytes. As shown in Fig. 9A, the compounds tested fell in three categories including weak partial activation (MBX-102 acid and SP1), partial activation (SP2, pioglitazone), or full activation (rosiglitazone, troglitazone, muraglitatar, and tesaglitazar) of FABP4 gene expression. MCP-1 secretion from LPS-stimulated primary mouse macrophages was used to profile the transrepression potential of each compound. Although all compounds significantly decreased MCP-1 secretion, the transrepression potential differed between compounds and was not correlated to their transactivation activity (Fig. 9B). As summarized in Fig. 9C, four separate categories of compounds could be identified based on the two-dimensional combination of their transactivation and transrepression abilities. Muraglitazar, troglitazone, and SP2 were both strong transactivators and transrepressors (TA/TR) whereas tesaglitazar, rosiglitazone, and pioglitazone were strong transactivators but weak transrepressors (TA/tr). Interestingly, although both SP1 and MBX-102 were equally weak

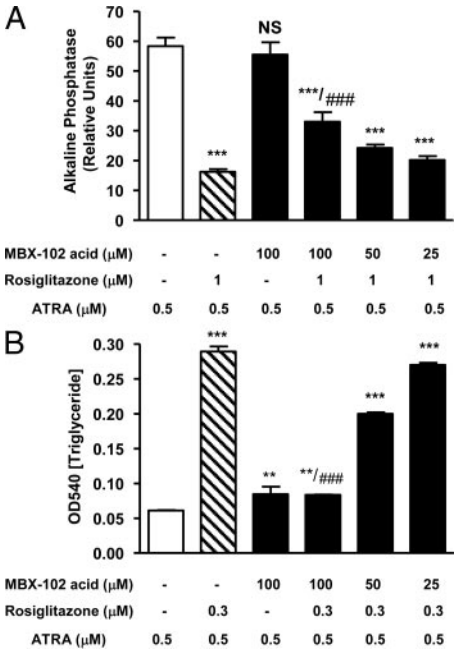

FIG. 7. Effect of MBX-102 acid on osteoblast/adipocyte differentiation pathways in murine C3H10T1/2 mesenchymal stem cells. A, Alkaline phosphatase activity. Rosiglitazone treatment significantly inhibited retinoic acid-stimulated alkaline phosphatase activity, whereas MBX-102 acid had no effect on this bone marker. B, Triglyceride deposition was dramatically increased by rosiglitazone treatment. MBX-102 acid had little effect on lipid accumulation and was able to fully antagonize the adipogenic capacity of rosiglitazone. Values are mean ± SEM and are representative of three independent experiments (**, $P <$ 0.01; ***, $P < 0.001$ *vs.* ATRA control; ###, $P < 0.001$ *vs.* rosiglitazone/ATRA-treated; one-way ANOVA and Tukey's multiple comparison test).

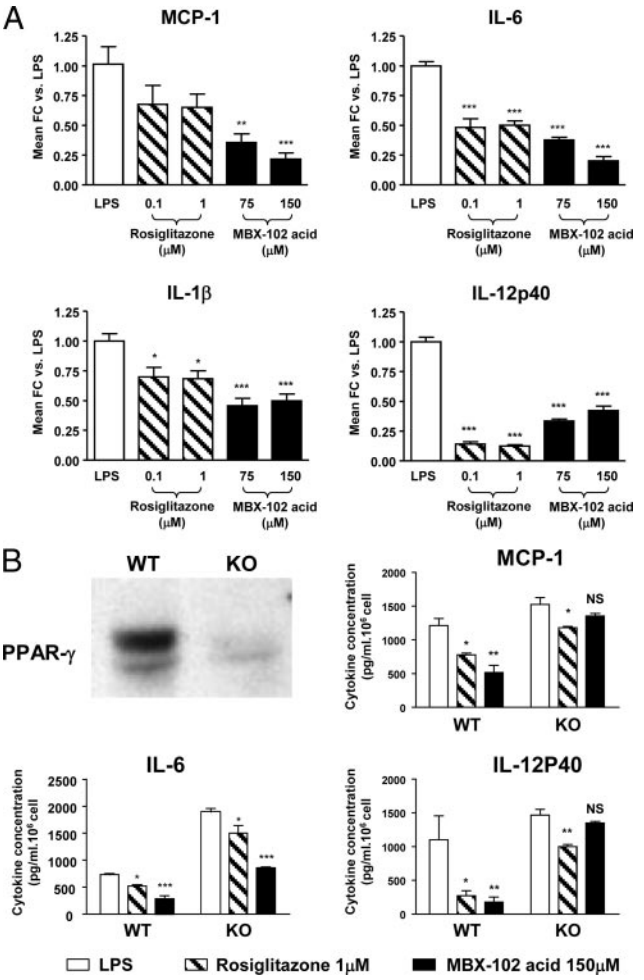

FIG. 8. A, LPS-induced MCP-1, IL-6, IL-1β, and IL12p40-secreted cytokine levels. B, WT or PPAR-γ −/− (KO) primary mouse macrophages. *Top left panel*, PPAR-γ protein levels. Values are mean ± SEM and represent either pooled data from two independent experiments (panel A) or mean ± SEM from a representative experiment (panel B) (*, $P < 0.05$; **, $P < 0.01$; ***, $P < 0.001$; one-way ANOVA and Tukey's multiple comparison test).

transactivators, they fell into two distinct categories because only MBX-102 displayed a strong ability to transrepress MCP-1 secretion (ta/TR), whereas SP1 was the weakest transrepressor (ta/tr).

Discussion

MBX-102 is the (−) enantiomer of halofenate and is currently in clinical development as a next generation insulin sensitizer. It displays glucose-lowering activity in diabetic patients (35), yet its mechanism of action is unclear. In this report, we provide evidence that MBX-102 is a selective partial agonist of PPAR-γ that differs from TZDs structurally, mechanistically, and preclinically. MBX-102 has a unique PPAR-γ activation profile and, in preclinical models, has potent insulin sensitization and antidiabetic activities without the side effects observed with PPAR-γ full agonists.

Our *in vitro* studies demonstrate that MBX-102 is a selective ligand and activator of PPAR-γ having no ability to activate either PPAR-α or PPAR-δ. MBX-102 is a partial PPAR-γ agonist that has weak transactivation potential and antagonizes rosiglitazone in cell-based settings. Binding to tyrosine 473 in helix 12 of the PPAR-γ LBD is required for the activity of full agonists, and absence of this interaction is a hallmark feature of partial PPAR-γ agonists (24, 32). Similar functional potency of MBX-102 acid with wild-type and mutated Y473A PPAR-γ in our reporter gene assay further supports its partial agonist status. These studies suggest that the binding site for MBX-102 acid in the PPAR-γ LBD overlaps with, but differs from, that of rosiglitazone, and we have confirmed this by solving the x-ray crystal structure of MBX-102 acid-bound PPAR-γ LBD (data not shown).

In vitro and *in vivo* studies demonstrate that MBX-102 is a potent insulin sensitizer and that short-term treatment with MBX-102 efficiently lowers glucose in several diabetic rodent models. Although commonly used for the assessment of partial PPAR-γ agonists (23, 36–40), short-term studies are not adequate for observing adverse events that require chronic drug exposure. Thus, long-term comparative studies are necessary to demonstrate an improved safety profile over the currently marketed drugs. In long-term studies in the insulin-resistant obese ZF rat model, MBX-102 treatment enhanced insulin sensitivity to a similar degree as rosiglitazone. Unlike rosiglitazone, MBX-102 did not affect body or heart weight and caused much smaller increases in adipose tissue masses, suggesting that MBX-102 possesses minimal adipogenic capacity *in vivo*.

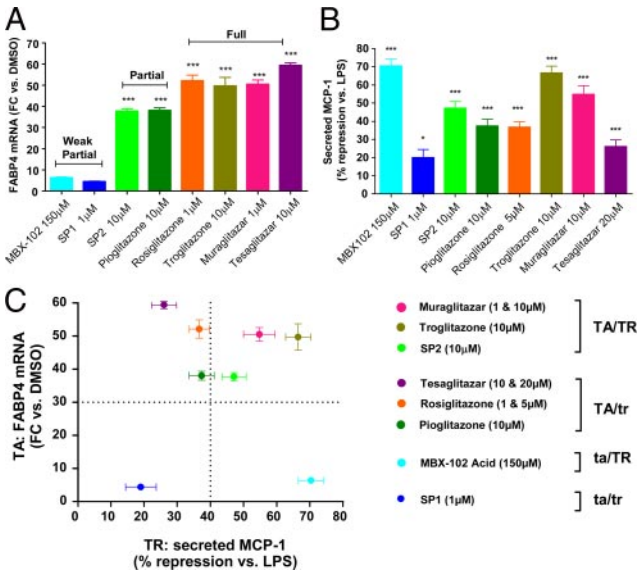

FIG. 9. Correlation between the transactivation and transrepression potential of several PPAR-γ (SP1, SP2, rosiglitazone, pioglitazone, troglitazone, and MBX-102 acid) and dual PPAR-α/γ (tesaglitazar and muraglitazar) agonists. The transactivation profile of each compound was assessed by measuring FABP4 gene induction and was plotted as fold change (FC) *vs.* the DMSO-treated control group. The transrepression profile was evaluated by assessing the ability of each compound to suppress MCP-1 secretion in LPS-stimulated mouse peritoneal macrophages and was plotted as percentage of suppression of MCP-1 secretion compared with the LPS DMSO-treated control group. Values are mean ± SEM and represent data obtained from one representative experiment (FABP4) or three independent experiments (MCP-1) (*, $P < 0.05$; **, $P < 0.01$; ***, $P < 0.001$ *vs.* control group; one-way ANOVA and Tukey's multiple comparison test).

This is in agreement with our *in vitro* data, which demonstrate that MBX-102 has reduced ability to drive murine and human adipogenesis and reduced ability to up-regulate key lipogenic genes in adipose cells. Because these effects on adipose tissue are characteristic of the full PPAR-γ agonists and are believed to be important for their insulin sensitization actions (41), our results raise an interesting question. In clinical and/or preclinical studies, treatment with TZDs have been shown to cause an adipose tissue remodeling, consisting of a decrease in intraabdominal fat and an increase in sc fat (42–47) that contains small, newly differentiated, insulin-responsive adipocytes (48, 49). Therefore, it would be of great interest to evaluate whether a partial PPAR-γ agonist such as MBX-102, which appears unable to change the overall adipose mass, also causes adipose tissue remodeling. Further studies are necessary to answer this question, including careful analysis of body composition, individual adipose depot mass, and adipocyte cell size distribution.

Exposure of rodent or human white adipocytes either in culture or *in vivo* to full PPAR-γ agonists leads to increased mitochondrial mass, induction of mitochondrial genes such as UCP-1, Cox8b, Cox7a1, and genes in the fatty acid oxidation pathway, resulting in enhanced oxygen consumption and lipid oxidation (50–52). Because both our *in vitro* and *in vivo* gene expression studies were rather limited, additional studies are needed to determine whether a partial PPAR-γ such as MBX-102 also has the ability to modulate the expression levels of these mitochondrial genes in adipose cells. Assessing whether MBX-102 treatment can positively modulate energy expenditure in future experiments would also be important.

Ligand-dependent nuclear hormone receptor activation turns on gene expression through the dissociation of corepressors and sequential recruitment of coactivators (5). PPAR-γ partial agonists have weaker coactivator recruitment activity compared with full agonists (23, 27). We have shown this is to be true for MBX-102 using FRET and ChIP analyses. Weak recruitment of coactivators by MBX-102 acid is not due to weak interaction of MBX-102 acid with PPAR-γ because MBX-102 acid induced efficient dissociation of the corepressors NCoR and SMRT. As proposed for other partial PPAR-γ agonists (8, 23), the markedly decreased adipogenic capacity of MBX-102 could be explained in part by its limited ability to recruit pro-adipogenic coactivators such as TIF2, CBP, P300, and TRAP220 (53). Differential coactivator recruitment is a likely mechanistic explanation for the differential gene expression profiles of MBX-102 and rosiglitazone.

The adipogenic activity of TZDs is associated with a reciprocal decrease in osteoblast differentiation and subsequent bone loss in rodents (8, 23, 54–58). Decreased *in vitro* adipogenic capacity is highlighted for most partial PPAR-γ agonists (4, 16, 23–27), but little information is available on their bone-related effects. Currently marketed TZDs have adverse skeletal actions that include decreased bone formation, accelerated bone loss, and increased risk of fracture (13–15, 59–61). Unlike rosiglitazone, MBX-102 has weak adipogenic activity in multipotent stem cells and, in these same cells, does not inhibit osteoblast differentiation. These data predict that the increase in fractures observed in women treated with TZDs will not be observed with MBX-102. Because PPAR-γ has recently been shown to regulate osteoclastogenesis in mice (62), preclinical investigations on the effects of MBX-102 on osteoclast differentiation and bone resorption are needed to better predict how MBX-102 will affect bone safety in a clinical setting.

Inflammation is a critical component in the pathogenesis of insulin resistance and the metabolic syndrome (63). Macrophages are a primary source of proinflammatory factors such as TNFα, IL-6, and MCP-1. Recent studies have shown that PPAR-γ plays an important role in the regulation of macrophage infiltration and activation in adipose tissue and atherosclerotic plaques (20, 21, 64), and TZDs have been shown to repress the expression of a number of nuclear factor-κB-dependent inflammatory genes (2, 22). MBX-102 is a potent transrepressor, and our data suggest this effect is partially PPAR-γ dependent and partially PPAR-γ independent, based on the cytokine assessed. Although activation of PPAR-δ by high concentrations of PPAR-γ agonists has been cited as a possible explanation for the PPAR-γ-independent repression of inflammatory genes in PPAR-γ-deficient macrophages (65), it can be ruled out here because MBX-102 has no ability to transactivate PPAR-δ in cell-based reporter assays. Surprisingly, rosiglitazone was able to partially transrepress the cytokines tested in our PPAR-γ-deficient macrophages. Although PPAR-γ protein was dramatically down-regulated in our knockout cells, we cannot claim it was fully abolished. Therefore, we cannot exclude the possibility that rosiglitazone was transrepressing inflammatory

genes through very low levels of remaining PPAR-γ protein in the knockout cells.

The molecular mechanisms by which MBX-102 transrepresses inflammatory mediators have yet to be established. PPAR-γ transrepresses inflammatory activation of macrophages by binding to nuclear receptor/corepressor complexes on the promoters of nuclear factor-κB target genes (22). Association of PPAR-γ at these sites requires ligand-dependent sumolyation and inhibits the exchange of corepressors for coactivators upon inflammatory stimulation. Thus, ligand-bound, sumolyated PPAR-γ transrepresses activation of inflammatory genes. For example, rosiglitazone and the partial agonist GW0072 both inhibit inflammation-induced inducible nitric oxide synthase expression and corepressor removal at the inducible nitric oxide synthase promoter (22). Although only rosiglitazone has been reported to induce PPAR-γ sumoylation, other transrepression-capable PPAR-γ ligands, such as MBX-102 acid, presumably induce PPAR-γ sumoylation as well.

One interesting aspect of this study relates to the transrepression ability of the various compounds tested. Our data demonstrate that strong transrepression activity is not necessarily a characteristic of partial selective PPAR-γ agonists. For example, SP1 is a weak transactivator and also a weak transrepressor. The unique profile of MBX-102 (*i.e.* weak transactivator and strong transrepressor) demonstrates, for the first time, that it is possible to separate transactivation and transrepression activities of PPAR-γ ligands and may explain why such a weak transactivator can retain full antidiabetic activity with reduced side effects.

Taken together, the evidence presented here strongly supports the claim that MBX-102 is an optimized, selective partial PPAR-γ agonist exhibiting full insulin sensitization activity with minimal adipogenic capacity both *in vitro* and *in vivo*. MBX-102 does not inhibit osteoblastogenesis or cause heart weight gain, highlighting its potential for lacking the negative skeletal and cardiovascular side effects seen with the currently marketed drugs. In agreement with these preclinical results, phase 2a clinical trial data indicate that MBX-102 significantly lowers plasma glucose levels in the absence of side effects such as weight gain and edema that are observed with the currently used pharmacological agents (35). This clinical trial was conducted using insulin-treated diabetic patients who are particularly sensitive to the TZD-induced side effects. Thus, these reported results obtained with MBX-102 are in stark contrast to those observed with the currently marketed TZDs. MBX-102 may therefore represents the next generation of insulin sensitizer and holds promising therapeutic potential in the treatment of type 2 diabetes.

Materials and Methods

Chemicals

MBX-102, SP1, SP2 (selective partial PPAR-γ agonist 2), rosiglitazone maleate, tesaglitazar, muraglitazar, and GW501516 were synthesized at Metabolex (Hayward, CA). Troglitazone and GW7647 were obtained from Sigma-Aldrich (St. Louis, MO).

Cell-based reporter assay

The LBD for human PPAR-γ (amino acids 172-476) was obtained by PCR and cloned into pFA-CMV plasmid (Stratagene, La Jolla, CA) to generate a Gal 4-human PPAR-γ LBD chimera. Gal4-human PPAR-γ Y473A LBD was generated by site-directed mutagenesis (QuikChange Site-Directed Mutagenesis Kit; Stratagene) as per manufacturer's instructions using the following oligonuclotides: forward: CGCTCCTGCAGGAGATCGCCAAGGACTTGTACTAG and reverse: CTAGTACAAGTCCTTGGCGATCTCCTGCAGGAGCG. HEK-293T cells were transfected with either Gal 4-human PPAR-γ LBD or Gal4-human PPAR-γ Y473A LBD, pFR-Luciferase, and Lac-z plasmids using Lipofectamine 2000 (Invitrogen, Carlsbad, CA) and incubated for 4 h before treatment with compound for 20–24 h. Expression was assayed using the Steady-Glo assay system (Promega Corp., Madison, WI) according to manufacturer's instructions. Fluorescence emission (excitation, 485 nm; emission, 535 nm) was measured after addition of 100 μl of 10 μM Fluorescein di-β-D-galactopyranoside (Invitrogen) in assay buffer (2.1 mM KH_2PO_4, 310.3 mM NaCl, 5.9 mM Na_2HPO_4-$7H_2O$, 20 mM KCl, 2 mM $MgSO_4$, 0.2% Triton X-100). Each experimental condition was performed in triplicate. The data were normalized for each well by dividing the luminescence measurement by the fluorescence measurement. Dose-response curves were generated and EC_{50} values were calculated using Prism version 5.01 (GraphPad Software, Inc., San Diego, CA).

Binding assay

The binding between test compounds and the human PPAR-γ LBD was measured using the PolarScreen PPAR-γ Competitor Assay (Invitrogen) using the manufacturer's recommended protocol.

FRET PPAR-γ coregulator peptide interaction assay

FRET PPAR-γ coregulator peptide interaction assays were performed using the LanthaScreen TR-FRET PPAR-γ Coactivator Assay Kit (catalog no. PV4548, Invitrogen, Carlsbad, CA) as per manufacturer's instructions. Human coregulator peptides were synthesized and conjugated to fluorescein by Invitrogen: Fl-TRAP220/DRIP (thyroid hormone receptor-associated protein 220, included in the PV4548 kit), Fl-CBP (catalog no. PV4596), Fl-PGC1α (catalog no. PV4421), Fl-SRC1 (nuclear receptor coactivator 1, catalog no. PV4582), Fl-TIF2/SRC2 (nuclear receptor coactivator 2, catalog no. PV4586), Fl-NCoR (NCoR 2, catalog no. PV4624), Fl-SMRT (silencing mediator for retinoid and thyroid-hormone receptors, catalog no. PV4423). MBX-102 acid or rosiglitazone was diluted to 2× in assay buffer and 10 μl was added to 384-well black plates. Glutathione-*S*-transferase-PPAR-γ LBD was diluted to 20 nM in assay buffer and 5 μl was added to the wells. A mixture of Tb anti-glutathione-*S*-transferase antibody (20 nM) and fluorescein-peptide (0.5 μM) was prepared in assay buffer and 5 μl was added to the wells. The plates were covered, shaken briefly, and incubated at room temperature for 4 h. TR-FRET signal was measured using a Pherastar fluorescence counter (BMG Labtech, Durham, NC). The data were calculated as the ratio of the emission intensity of the acceptor (fluorescein: λ = 520 nm) divided by the emission intensity of the donor (Tb: λ = 490 nm). Dose-response curves for each coregulator were done in quadruplicate and the EC_{50}/IC_{50} values were generated using Prism version 5.01 (GraphPad). Coactivator data were analyzed as a percentage of the maximum rosiglitazone response. Corepressor data were analyzed as a percentage of the maximum recruitment in the absence of ligand. Experiments for CBP, PGC1α, SRC1, and NCoR were repeated twice (n = 2). Experiments for TRAP220 and TIF2 were repeated four times (n = 4). Experiments for SMRT were repeated five times (n = 5).

Glucose uptake and gene silencing in 3T3-L1 adipocytes

Cell culture and electroporation

3T3-L1 fibroblasts were plated into growth medium [DMEM supplemented with 10% fetal bovine serum (FBS), 1% penicillin-streptomycin] and grown to confluence for 7 d, with media changes every 2–3

d. Differentiation into adipocytes was induced by incubating the cells in DMEM supplemented with 10% FBS, 1% penicillin-streptomycin, 698 nM bovine insulin, 518 μM IBMX, and 248 nM dexamethasone. 3T3-L1 adipocytes (4 d of age) were transfected with siRNA duplexes by electroporation. PPAR-γ P17 siRNA sequence was derived from Katayama *et al.* (66), and siRNA duplexes, including a scramble control siRNA, were synthesized by Dharmacon (Lafayette, CO). Briefly, 4-d-old differentiated adipocytes were electroporated with 10 nmol of PPAR-γ P17 siRNA duplexes or 10 nmol of scramble control siRNA duplexes using a BTX generator 830 electroporator (settings: 170 V, 7 msec, two pulses). After electroporation, cells were resuspended in 4 ml of DMEM/10% medium, counted and plated into 96-well plates (for glucose uptake assay) or 24-well plates (for cell viability and protein and RT-PCR analysis). Electroporated cells were incubated for 8 h at 37 C, 8% CO_2. The cells were then treated for 16 h with DMSO, MBX-102 acid (100 μM), rosiglitazone (1 μM), or Endothelin-1 (ET-1, 1 nM, obtained from Sigma-Aldrich) prepared in DMEM/10% FBS media. The final concentration of DMSO in all treatments was 0.05%.

2-Deoxy-D-[^{3}H] glucose uptake assay

Glucose uptake activity was determined by measuring the uptake of 2-deoxy-D-[^{3}H] glucose (Amersham/GE, Piscataway, NJ). Briefly, 3T3-L1 adipocytes (electroporated and compound treated as above) were washed once with PBS, two times with fat cell buffer (FCB: 125 mM NaCl, 5 mM KCl, 1.8 mM $CaCl_2$, 2.6 mM $MgSO_4$, 25 mM HEPES, 2 mM pyruvate and 2% BSA, 0.2 μm sterile filtered) and were serum starved by incubation with FCB at 37 C for 30 min. Insulin was prepared at the indicated concentrations in FCB, added to the cells, and incubated for 20 min at 37 C. Glucose uptake was initiated by the addition of 2-deoxy-D-[^{3}H] glucose (0.083 μCi/ml) and 1.1 mM 2-deoxy-D-glucose (Sigma-Aldrich) in FCB and incubated for 10 min at 37 C. Glucose uptake was terminated by removing the contents of the wells and washing the cells three times with cold PBS. The cells were disrupted with scintillation solution, and 2-deoxy-D-[^{3}H] glucose retained by the cells was counted (MicroBeta TriLux 1450; PerkinElmer, Boston, MA). Cell viability was assessed independently with the CellTitre-Glo Luminescent Cell Viability Assay Kit (Promega, Madison, WT) as per manufacturer's instructions. Glucose uptake was quantified by normalizing the glucose uptake measurement for each compound treatment to the corresponding cell viability value. The fold induction of glucose uptake was calculated by normalizing all values against the average value of the scramble control basal value (taken as 1-fold).

PPAR-γ protein levels

After experimental treatments, PPAR-γ and actin levels were assessed by Western blot using anti-PPAR-γ antibodies [1:200 dilution, rabbit polyclonal anti-human PPAR-γ (sc-7196), Santa Cruz Biotechnology (Santa Cruz, CA)] or antiactin, horseradish peroxidase (HRP) antibodies (1:250 dilution, goat polyclonal anti-Actin, HRP conjugated (sc-1616), Santa Cruz Biotechnology) followed by antirabbit, HRP antibodies [1:3000 dilution, goat polyclonal antirabbit, HRP antibody; Jackson ImmunoResearch Laboratories (West Grove, PA)].

PPAR-γ mRNA levels determination

Cells were harvested using Trizol (Invitrogen) and total RNA was prepared. cDNA was prepared by reverse transcription and Taqman (RT-PCR) was performed using gene expression assay mixes (ABI, Foster City, CA) for PPAR-γ (Mm00440945_m1) and the acidic ribosomal phosphoprotein P0 (Arbp, Mm00725448_s1).

Human preadipocyte differentiation study

Cultured human preadipocytes (Lot no. L060403T; Zen-Bio, Inc., Research Triangle Park, NC) were incubated in differentiation medium (catalog no. DM-2, without PPAR-γ agonist, Zen-Bio, Inc.) in the presence of either vehicle (DMSO 0.2%), rosiglitazone (1 μM), or MBX-102 acid (10, 50, 100, or 200 μM) for 3 d. Cells were then fed with Adipocyte Medium (catalog no. AM-1, containing 100 nM insulin and 1.0 μM dexamethasone, without DMSO or compound) for an additional 12 d. At d 15, PPAR-γ-mediated ligand-induced differentiation was assessed either by analysis of total triglyceride or Oil-red-O staining.

Human adipocyte cultures and treatment for gene expression analysis

Differentiated human adipocytes were obtained from Zen-Bio and were treated for 48 h with DMSO (0.1%), MBX-102 acid (100 μM), or rosiglitazone (1 μM). After treatment, the cells were harvested for gene expression analysis using a quantitative nuclease protection technology (HTG, Inc., Tucson, AZ). Briefly, the cells were harvested with HTG proprietary lysis buffer, and cell lysates were shipped to HTG for mRNA measurement on a custom quantitative nuclease protection multiplex array. Two independent experiments were performed using two different cell lots (lots L042503abd and L060403T). Final results were pooled, and the fold change *vs.* vehicle was calculated for each compound treatment.

Mouse adipocyte cultures and treatment for gene expression analysis

3T3-L1 adipocytes (d 7 after differentiation) were replated in 24-well plates and treated with vehicle (DMSO 0.1%), MBX-102 acid (150 μM), or rosiglitazone (1 μM) for 24 h. Total RNA was isolated, and RT-PCR (Taqman) was performed as described above using the following ABI gene expression assay mixes for glycerol kinase (GyK, Mm00433907_m1), phosphoenolpyruvate carboxykinase (PEPCK, Mm00440636_m1), (FABP4, Mm00445880_m1), the thrombospondin receptor (CD36, Mm00432403_m1), 11β-hydroxysteroid dehydrogenase type 1 (HSD11B1, Mm00476182_m1), pyruvate dehydrogenase kinase 4 (Mm00443325_m1), angiopoietin-like 4 (ANGPTL4,Mm00480431_m1) or Arbp (catalog no. Mm00725448_s1). The fold change *vs.* vehicle in gene expression was calculated using the comparative C_t method for relative quantitation. Each compound was tested in at least six replicate wells.

ChIP study

Differentiated 3T3-L1 adipocytes were treated for 48 h with DMSO, rosiglitazone (1 μM), or MBX-102 acid (150 μM). Assays were performed according to the protocol provided with the Upstate EZ ChIP kit (Upstate Biotechnology, Lake Placid, NY; catalog no. 17-371). Briefly, cells were cross-linked with 1% (vol/vol) formaldehyde in PBS for 10 min, lysed in 1% (wt/vol) sodium dodecyl sulfate, and sonicated. Cell lysates were precleared with protein A-agarose for 1 h at 4 C, and the cleared supernatant was incubated with 5 μg of each antibody directed against PPAR-γ (Santa Cruz, H-100), NCoR [equal mix of ab24552 (Abcam) and H-303 and C-20 (Santa Cruz)], SMRT (equal mix of Abcam, ab5800 and ab24551), p300 (Santa Cruz N-15), CBP (equal mix of Santa Cruz A-22, C-20, and 451), TRAP220 (equal mix of Santa Cruz M-255, C-19, and S-19), or acetylhistone H4 rabbit polyclonal antiserum at 4 C overnight. Immune complexes were recovered with salmon sperm DNA/protein A-agarose slurry. After washing, genomic DNA was extracted (by reverse cross-linking and purification using spin columns) and used as template for PCR with the following mouse-specific primers: GyK: forward, 5′-CGGAATTCTGATCCCTACTGTGC-3′; reverse, 5′-GACACTAGGCCAACTTCTCTGTCAA-3′. PEPCK: forward, 5′-GAACTCCGACAAGCAAGCTCTCAGC-3′; reverse, 5′-CCCAAGTGTCTGGAGAAAGGAGG-3′. PCR was performed using the PfuTurbo PCR Master Mix (Stratagene, La Jolla, CA, as per manufacturer's instructions). Resulting DNA fragments were visualized by ethidium bromide gel electrophoresis.

Osteoblast/adipocyte differentiation pathways in murine C3H10T1/2 mesenchymal cells

The pluripotent stem cell line C3H10 T1/2 was obtained from ATCC (ATCC catalog no. CCL-226). Cells were maintained at subconfluent density in DMEM supplemented with 10% FBS, 1% penicillin/streptomycin up to passage 20. To measure the effect of compounds on

lipogenesis (adipogenic marker) and alkaline phosphatase activity (early osteoblast marker), cells were seeded in 96-well plates at a density of 10,000 cells per well. Two days after reaching confluence the cells were treated with 200 nM insulin, 500 nM ATRA (Sigma-Aldrich) and varying concentrations of compound. Fresh media and compounds were added at d 4, and lipogenesis and alkaline phosphatase activity was assessed at d 8. At d 8 cells were washed with PBS followed by hypotonic lysis in the presence of 1% Triton X-100 at 4 C for determining alkaline phosphatase (ALP) activity. For triglyceride accumulation, cells were lysed in 1% digitonin (Sigma-Aldrich) after being washed in PBS. Total triglyceride accumulation was determined using Trident reagent (Sigma-Aldrich) by measuring absorbance at 540 nm. Alkaline phosphatase activity was measured using *p*-nitrophenol as a substrate (phosphatase substrate, (Sigma-Aldrich) by measuring absorbance at 405 nm. Cell density and viability were measured with a nonradioactive cell proliferation assay [CellTiter 96 Non-Radioactive Cell Proliferation Assay (Promega Corp., Madison, WI].

In vivo studies

The Metabolex Institutional Animal Care and Use Committee approved all animal care and experimental procedures described below. All animals were housed in temperature (22 ± 3 C) and humidity (55 ± 4%) controlled rooms, with 12-h light (0600–1800 h)/dark cycle. Unless specified otherwise, mice were housed four to five mice per cage, and rats were housed two rats per cage and were allowed *ad libitum* access to tap water and Purina Rodent Chow (stock no. 5001 4.5% fat; Nestle Purina, St. Louis, MO).

Reagents and assays

Plasma glucose levels were measured using the method of Trinder (Glucose Oxidase G7016; Peroxidase P8125; Sigma Chemical Co.). Plasma triglycerides were measured using a triglyceride diagnostic kit (kit 344, Sigma Chemical Co.), plasma insulin and adiponectin levels were determined using a rat Insulin EIA kit (catalog no. 80-INSRTU-E10; ALPCO Diagnostics, Salem, NH) and rat adiponectin EIA Kit (catalog no. 44-ADPRT-E01; ALPCO Diagnostics) respectively, according to the instructions provided by the manufacturer.

Short-term in vivo efficacy studies

For the ob/ob study, 8-wk-old male *ob/ob* mice (The Jackson Laboratory, Bar Harbor, ME) were used. Vehicle (5 ml/kg, 1% carboxymethyl cellulose), rosiglitazone maleate (10 mg/kg), or MBX-102 (125 mg/kg) was administered by oral gavage daily for 12 d. For the *db/db* study, 11-wk-old male *db/db* mice were used. Vehicle (5 ml/kg), rosiglitazone maleate (10 mg/kg), or MBX-102 (250 mg/kg) was administered by oral gavage for 9 d. For the ZDF rat study, 9-wk-old male ZDF rats (Charles River Laboratories, Inc., Wilmington, MA) were used. Vehicle (5 ml/kg), rosiglitazone maleate (4 mg/kg), or MBX-102 (100 mg/kg) was administered by oral gavage for 11 d. At the end of treatment, blood samples were collected after a 6 h fast by tail nip.

Clamp studies

Male ZDF rats were obtained from Harlan Laboratories (San Diego, CA) at 8 wk of age. ZDF rats were single housed and allowed access *ad libitum* to tap water and chow (Purina 5008 diet; Ralston Purina Co., St. Louis, MO). ZDF rats were screened into three groups with similar mean plasma glucose levels. ZDF rats were cannulated in the jugular vein and the carotid artery and were allowed to recover at least for 2 d. Rats were dosed with either vehicle or MBX-102 (100 mg/kg) by oral gavage for 4–7 d. On the day of the clamp experiment, rats were dosed and food was withdrawn 1 h later. After rats were fasted for 4 h, blood samples were taken from the carotid catheter to measure basal glucose and insulin levels. Experiments were initiated with a priming injection (0.5 ml/rat of 5 μCi/ml of D-[3-^{3}H] glucose) and initiation of a constant infusion of D-[3-^{3}H] glucose tracer (8 μCi/ml) at a rate of 10 μl/min for 60 min. After the 1-h tracer-equilibration period, a post-tracer blood sample was collected for glucose, insulin and D-[3-^{3}H] glucose specific activity (SA) measurements. Infusion of tracer glucose was then discontinued, and insulin infusion was initiated (10 μl/min equivalent to 40 mU/kg/min) along with glucose infusion. The glucose infusion rate was adjusted empirically to achieve plasma glucose level at 150 mg/dl ± 5% within the next 1.5–2 h. To facilitate this process, blood samples were collected at 10-min intervals for immediate plasma glucose measurements using a glucometer until the end of the study. Clamp was defined by three consecutive glucose measurements that were within the above defined range. Samples (300–400 μl) at the three time points (10-min interval) were collected for glucose, insulin, and D-[3-^{3}H] glucose SA measurements.

In vivo chronic efficacy study

Male 9-wk-old Zucker Lean (ZL) and Zucker Fatty (ZF) rats were obtained from Charles River Laboratories. Vehicle and drug suspensions were administered to the rats daily by oral gavage for 50 d. Eight rats were assigned to each of the following groups: ZL Vehicle (5 ml/kg), ZF Vehicle (5 ml/kg), ZF + rosiglitazone maleate (0.3, 1, 3, 10, and 30 mg/kg) and ZF + MBX-102 (3, 10, 30, 60, and 100 mg/kg). Body weight and food intake were recorded every 2–4 d. An oral glucose tolerance test was performed at d 43 of dosing (supplemental Fig. 4 and supplemental methods). Blood samples (~250 μl) were collected to measure plasma glucose and insulin levels. The insulin resistance index was calculated by multiplying glucose by insulin values (glucose × insulin) at each time point. The glucose and insulin area under the curves were calculated according to the trapezoidal rule. The insulin resistance area under the curve was calculated by applying the trapezoidal rule to the insulin resistance index values obtained for each time point, as described above. Blood and tissue samples were collected at study end (d 51) by cardiac puncture after a 6-h fast to measure insulin, triglycerides, and adiponectin.

Mouse peritoneal macrophages and 3T3-L1 preadipocyte cultures

Cytokine secretion studies in mouse peritoneal macrophages

Mouse peritoneal macrophages were obtained from C57BL/6J male mice following 3 d of thioglycolate stimulation. Isolated macrophages were cultured for 2 d in RPMI 1640, 10% FBS and followed by serum starvation in DMEM + 0.5% FBS overnight. Then the macrophages were treated in DMEM for 1 h with either vehicle (DMSO), MBX-102 acid (150 μM), or rosiglitazone (1.0 μM) followed by stimulation with 100 ng/ml LPS for 24 h. Cell supernatants were then harvested and stored at −20 C before analysis of secreted cytokine levels using a Procarta Cytokine Profiling Kit (Panomics Inc,. Fremont, CA). The experiment was performed twice with each experimental condition run in quadruplicate. The fold change relative to LPS data from the replicate experiments were pooled for statistical analysis. PPAR-γ −/− (KO) macrophages were obtained by crossing PPAR-γ f/f mice with MX-Cre transgenic mice as previously described (65).

FABP4 gene expression studies in 3T3-L1 preadipocytes

Cryo-preserved 3T3-L1 preadipocytes were thawed, placed into culture media (DMEM/10% FBS/1% Pen-Strep), plated into 150-mm cell culture dishes, and allowed to grow to confluence for 7 d. The cells were then trypsinized, placed into DMEM/10% FBS, replated into 24-well plates at a density of 25,000 cells per well, and incubated 18–24 h at 37 C, 8% CO_2. The following day, test compounds were prepared at 2× concentration in DMEM/10% FBS. Medium was aspirated from the cells and 250 μl/well fresh DMEM/10% FBS followed by 250 μl/well 2× compound was added to the wells. The final concentration of DMSO was 0.1% in all conditions tested. The cells were incubated with compound for 72 h and then harvested in Qiazol Lysis Reagent (QIAGEN, Chatsworth, CA). Total RNA was isolated and RT-PCR (Taqman) was performed as described above using the following ABI

gene expression assay mixes for FABP4 (catalog no. Mm00445880_m1) and Arbp (catalog no. Mm00725448_s1).

Statistical analysis

Data are expressed as mean ± SEM. Prism software (GraphPad version 5.01) was used for all statistical analysis. Unless specified otherwise in the figure legends, one-way ANOVA followed by Tukey's or Dunnett's multiple comparison tests, or two-way ANOVA followed by Bonferroni post tests was used to assess statistical differences between groups. When appropriate, an unpaired, two-tailed *t* test was performed. All *P* values < 0.05 were considered statistically significant (NS or ns, $P > 0.05$; *, $P < 0.05$; **, $P < 0.01$; and ***, $P < 0.001$).

Acknowledgments

We thank Carl Mondon, Vanina Barreiro, Bindu Pandey, James Tang, Apurva Chandalia, and Judy Udove (Metabolex, Inc., Hayward, CA) for excellent technical assistance with the *in vivo* studies. We thank Andrea Bell, Zhonghao Liu, and Paul Lee (Metabolex, Inc.) for their help with the *in vitro* studies. We thank Jerry Olefsky (University of California San Diego) and Morris Birnbaum (University of Pennsylvania, Philadelphia, PA) for their insightful review of the manuscript.

Address all correspondence and requests for reprints to: Dr. Brian Lavan, Department of Biology, Metabolex, 3876 Bay Center Place, Hayward, California 94545. E-mail: blavan@metabolex.com.

Present address for H.J.C.: Department of Molecular Biology, Genentech, Inc., 1 DNA Way, South San Francisco, California 94080.

Disclosure Summary: F.M.G. is employed by Metabolex, Inc. and has an equity interest in Metabolex, Inc. F.Z. was previously employed by Metabolex, Inc. and has an equity interest in Metabolex Inc. Y.M. and B.E.L. are currently employed by Metabolex, Inc. H.J.C., T.A.G., and L.E.C. were formerly employed by Metabolex, Inc. D.D.S. and S.F. received research support from Metabolex, Inc. directly related to this manuscript. J.L. and D.R. are employees of Johnson & Johnson, Inc. and hold equity interests in Johnson & Johnson, Inc.

References

1. **Lecka-Czernik B, Moerman EJ, Grant DF, Lehmann JM, Manolagas SC, Jilka RL** 2002 Divergent effects of selective peroxisome proliferator-activated receptor-γ 2 ligands on adipocyte *versus* osteoblast differentiation. Endocrinology 143:2376–2384
2. **Ricote M, Glass CK** 2007 PPARs and molecular mechanisms of transrepression. Biochim Biophys Acta 1771:926–935
3. **Kliewer SA, Sundseth SS, Jones SA, Brown PJ, Wisely GB, Koble CS, Devchand P, Wahli W, Willson TM, Lenhard JM, Lehmann JM** 1997 Fatty acids and eicosanoids regulate gene expression through direct interactions with peroxisome proliferator-activated receptors α and γ. Proc Natl Acad Sci USA 94:4318–4323
4. **Rubenstrunk A, Hanf R, Hum DW, Fruchart JC, Staels B** 2007 Safety issues and prospects for future generations of PPAR modulators. Biochim Biophys Acta 1771:1065–1081
5. **Rosenfeld MG, Lunyak VV, Glass CK** 2006 Sensors and signals: a coactivator/corepressor/epigenetic code for integrating signal-dependent programs of transcriptional response. Genes Dev 20:1405–1428
6. **Glass CK, Rosenfeld MG** 2000 The coregulator exchange in transcriptional functions of nuclear receptors. Genes Dev 14:121–141
7. **Nolte RT, Wisely GB, Westin S, Cobb JE, Lambert MH, Kurokawa R, Rosenfeld MG, Willson TM, Glass CK, Milburn MV** 1998 Ligand binding and coactivator assembly of the peroxisome proliferator-activated receptor-γ. Nature 395:137–143
8. **Burgermeister E, Schnoebelen A, Flament A, Benz J, Stihle M, Gsell B, Rufer A, Ruf A, Kuhn B, Märki HP, Mizrahi J, Sebokova E, Niesor E, Meyer M** 2006 A novel partial agonist of peroxisome proliferator-activated receptor-γ (PPARγ) recruits PPARγ-coactivator-1α, prevents triglyceride accumulation, and potentiates insulin signaling *in vitro*. Mol Endocrinol 20:809–830
9. **Einstein M, Akiyama TE, Castriota GA, Wang CF, McKeever B, Mosley RT, Becker JW, Moller DE, Meinke PT, Wood HB, Berger JP** 2008 The differential interactions of peroxisome proliferator-activated receptor γ ligands with Tyr473 is a physical basis for their unique biological activities. Mol Pharmacol 73:62–74
10. **Oberfield JL, Collins JL, Holmes CP, Goreham DM, Cooper JP, Cobb JE, Lenhard JM, Hull-Ryde EA, Mohr CP, Blanchard SG, Parks DJ, Moore LB, Lehmann JM, Plunket K, Miller AB, Milburn MV, Kliewer SA, Willson TM** 1999 A peroxisome proliferator-activated receptor γ ligand inhibits adipocyte differentiation. Proc Natl Acad Sci USA 96:6102–6106
11. **Picard F, Auwerx J** 2002 PPARγ and glucose homeostasis. Annu Rev Nutr 22:167–197
12. **Gurnell M, Savage DB, Chatterjee VK, O'Rahilly S** 2003 The metabolic syndrome: peroxisome proliferator-activated receptor γ and its therapeutic modulation. J Clin Endocrinol Metab 88:2412–2421
13. **Grey A** 2008 Skeletal consequences of thiazolidinedione therapy. Osteoporos Int 19:129–137
14. **Meier C, Kraenzlin ME, Bodmer M, Jick SS, Jick H, Meier CR** 2008 Use of thiazolidinediones and fracture risk. Arch Intern Med 168:820–825
15. **Schwartz AV** 2008 TZDs and bone: a review of the recent clinical evidence. PPAR Res 2008:297893
16. **Shearer BG, Billin AN** 2007 The next generation of PPAR drugs: do we have the tools to find them? Biochim Biophys Acta 1771:1082–1093
17. **Pascual G, Sullivan AL, Ogawa S, Gamliel A, Perissi V, Rosenfeld MG, Glass CK** 2007 Anti-inflammatory and antidiabetic roles of PPARγ. Novartis Found Symp 286:183–196; discussion 196–203
18. **Straus DS, Glass CK** 2007 Anti-inflammatory actions of PPAR ligands: new insights on cellular and molecular mechanisms. Trends Immunol 28:551–558
19. **Széles L, Töröcsik D, Nagy L** 2007 PPARγ in immunity and inflammation: cell types and diseases. Biochim Biophys Acta 1771:1014–1030
20. **Hevener AL, Olefsky JM, Reichart D, Nguyen MT, Bandyopadyhay G, Leung HY, Watt MJ, Benner C, Febbraio MA, Nguyen AK, Folian B, Subramaniam S, Gonzalez FJ, Glass CK, Ricote M** 2007 Macrophage PPAR γ is required for normal skeletal muscle and hepatic insulin sensitivity and full antidiabetic effects of thiazolidinediones. J Clin Invest 117:1658–1669
21. **Odegaard JI, Ricardo-Gonzalez RR, Goforth MH, Morel CR, Subramanian V, Mukundan L, Red Eagle A, Vats D, Brombacher F, Ferrante AW, Chawla A** 2007 Macrophage-specific PPARγ controls alternative activation and improves insulin resistance. Nature 447:1116–1120
22. **Pascual G, Fong AL, Ogawa S, Gamliel A, Li AC, Perissi V, Rose DW, Willson TM, Rosenfeld MG, Glass CK** 2005 A SUMOylation-dependent pathway mediates transrepression of inflammatory response genes by PPAR-γ. Nature 437:759–763
23. **Carmona MC, Louche K, Lefebvre B, Pilon A, Hennuyer N, Audinot-Bouchez V, Fievet C, Torpier G, Formstecher P, Renard P, Lefebvre P, Dacquet C, Staels B, Casteilla L, Pénicaud L** 2007 S 26948: a new specific peroxisome proliferator activated receptor γ modulator with potent antidiabetes and antiatherogenic effects. Diabetes 56:2797–2808
24. **Einstein M, Akiyama TE, Castriota GA, Wang CF, McKeever B, Mosley R, Becker JW, Moller DE, Meinke PT, Wood HB, Berger JP** 2008 The differential interactions of PPARγ ligands with tyrosine 473 is a physical basis for their unique biological activities. Mol Pharmacol 73:62–74
25. **Gelman L, Feige JN, Desvergne B** 2007 Molecular basis of selective PPARγ modulation for the treatment of type 2 diabetes. Biochim Biophys Acta 1771:1094–1107
26. **Chang F, Jaber LA, Berlie HD, O'Connell MB** 2007 Evolution of peroxisome proliferator-activated receptor agonists. Ann Pharmacother 41:973–983
27. **Zhang F, Lavan BE, Gregoire FM** 2007 Selective modulators of PPAR-γ activity: molecular aspects related to obesity and side-effects. PPAR Res 2007:32696
28. **Aronow WS, Vangrow JS, Nelson WH, Pagano J, Papageorge's NP, Khursheed M, Harding PR, Khemka M** 1973 Halofenate: an effective hypolipemia- and hypouricemia-inducing drug. Curr Ther Res Clin Exp 15:902–906
29. **Feldman EB, Gluck FB, Carter AC** 1978 Effects of halofenate on glucose tolerance in patients with hyperlipoproteinemia. J Clin Pharmacol 18:241–248
30. **Krut LH, Seftel HC, Joffe BI** 1977 Comparison of clofibrate with halofenate in diabetics with hyperlipidaemia. S Afr Med J 51:348–352
31. **Allen T, Zhang F, Moodie SA, Clemens LE, Smith A, Gregoire F, Bell A, Muscat GE, Gustafson TA** 2006 Halofenate is a selective peroxisome proliferator-activated receptor γ modulator with antidiabetic activity. Diabetes 55:2523–2533
32. **Bruning JB, Chalmers MJ, Prasad S, Busby SA, Kamenecka TM, He Y, Nettles KW, Griffin PR** 2007 Partial agonists activate PPARγ using a helix 12 independent mechanism. Structure 15:1258–1271

33. **Arakawa K, Ishihara T, Aoto M, Inamasu M, Kitamura K, Saito A** 2004 An antidiabetic thiazolidinedione induces eccentric cardiac hypertrophy by cardiac volume overload in rats. Clin Exp Pharmacol Physiol 31:8–13
34. **Yu S, Reddy JK** 2007 Transcription coactivators for peroxisome proliferator-activated receptors. Biochim Biophys Acta 1771:936–951
35. **Rosenstock J, Flores-Lozano F, Schartz S., Gonzalez-Galvez G, Karpf D** 2005 MBX-102: a novel non-TZD insulin sensitizer that improves glycemic control without causing edema or weight gain in patients with type 2 diabetes (T2DM) on concomitant insulin therapy. Diabetes 54:44-OR (Abstract)
36. **Fukui Y, Masui S, Osada S, Umesono K, Motojima K** 2000 A new thiazolidinedione, NC-2100, which is a weak PPAR-γ activator, exhibits potent antidiabetic effects and induces uncoupling protein 1 in white adipose tissue of KKAy obese mice. Diabetes 49:759–767
37. **Kim KR, Lee JH, Kim SJ, Rhee SD, Jung WH, Yang SD, Kim SS, Ahn JH, Cheon HG** 2006 KR-62980: A novel peroxisome proliferator-activated receptor γ agonist with weak adipogenic effects. Biochem Pharmacol 72:446–454
38. **Ostberg T, Svensson S, Selén G, Uppenberg J, Thor M, Sundbom M, Sydow-Bäckman M, Gustavsson AL, Jendeberg L** 2004 A new class of peroxisome proliferator-activated receptor agonists with a novel binding epitope shows antidiabetic effects. J Biol Chem 279:41124–41130
39. **Reginato MJ, Bailey ST, Krakow SL, Minami C, Ishii S, Tanaka H, Lazar MA** 1998 A potent antidiabetic thiazolidinedione with unique peroxisome proliferator-activated receptor γ-activating properties. J Biol Chem 273:32679–32684
40. **Rocchi S, Picard F, Vamecq J, Gelman L, Potier N, Zeyer D, Dubuquoy L, Bac P, Champy MF, Plunket KD, Leesnitzer LM, Blanchard SG, Desreumaux P, Moras D, Renaud JP, Auwerx J** 2001 A unique PPARγ ligand with potent insulin-sensitizing yet weak adipogenic activity. Mol Cell 8:737–747
41. **Bays H, Mandarino L, DeFronzo RA** 2004 Role of the adipocyte, free fatty acids, and ectopic fat in pathogenesis of type 2 diabetes mellitus: peroxisomal proliferator-activated receptor agonists provide a rational therapeutic approach. J Clin Endocrinol Metab 89:463–478
42. **Miyazaki Y, Glass L, Triplitt C, Matsuda M, Cusi K, Mahankali A, Mahankali S, Mandarino LJ, DeFronzo RA** 2001 Effect of rosiglitazone on glucose and non-esterified fatty acid metabolism in type II diabetic patients. Diabetologia 44:2210–2219
43. **Miyazaki Y, Glass L, Triplitt C, Wajcberg E, Mandarino LJ, DeFronzo RA** 2002 Abdominal fat distribution and peripheral and hepatic insulin resistance in type 2 diabetes mellitus. Am J Physiol Endocrinol Metab 283:E1135–E1143
44. **Miyazaki Y, Mahankali A, Matsuda M, Mahankali S, Hardies J, Cusi K, Mandarino LJ, DeFronzo RA** 2002 Effect of pioglitazone on abdominal fat distribution and insulin sensitivity in type 2 diabetic patients. J Clin Endocrinol Metab 87:2784–2791
45. **Mori Y, Murakawa Y, Okada K, Horikoshi H, Yokoyama J, Tajima N, Ikeda Y** 1999 Effect of troglitazone on body fat distribution in type 2 diabetic patients. Diabetes Care 22:908–912
46. **Kawai T, Takei I, Oguma Y, Ohashi N, Tokui M, Oguchi S, Katsukawa F, Hirose H, Shimada A, Watanabe K, Saruta T** 1999 Effects of troglitazone on fat distribution in the treatment of male type 2 diabetes. Metabolism 48:1102–1107
47. **Kelly IE, Han TS, Walsh K, Lean ME** 1999 Effects of a thiazolidinedione compound on body fat and fat distribution of patients with type 2 diabetes. Diabetes Care 22:288–293
48. **Boden G, Cheung P, Mozzoli M, Fried SK** 2003 Effect of thiazolidinediones on glucose and fatty acid metabolism in patients with type 2 diabetes. Metabolism 52:753–759
49. **Okuno A, Tamemoto H, Tobe K, Ueki K, Mori Y, Iwamoto K, Umesono K, Akanuma Y, Fujiwara T, Horikoshi H, Yazaki Y, Kadowaki T** 1998 Troglitazone increases the number of small adipocytes without the change of white adipose tissue mass in obese Zucker rats. J Clin Invest 101:1354–1361
50. **Bogacka I, Ukropcova B, McNeil M, Gimble JM, Smith SR** 2005 Structural and functional consequences of mitochondrial biogenesis in human adipocytes *in vitro*. J Clin Endocrinol Metab 90:6650–6656
51. **Bogacka I, Xie H, Bray GA, Smith SR** 2005 Pioglitazone induces mitochondrial biogenesis in human subcutaneous adipose tissue in vivo. Diabetes 54:1392–1399
52. **Wilson-Fritch L, Nicoloro S, Chouinard M, Lazar MA, Chui PC, Leszyk J, Straubhaar J, Czech MP, Corvera S** 2004 Mitochondrial remodeling in adipose tissue associated with obesity and treatment with rosiglitazone. J Clin Invest 114:1281–1289
53. **Feige JN, Auwerx J** 2007 Transcriptional coregulators in the control of energy homeostasis. Trends Cell Biol 17:292–301
54. **Ali AA, Weinstein RS, Stewart SA, Parfitt AM, Manolagas SC, Jilka RL** 2005 Rosiglitazone causes bone loss in mice by suppressing osteoblast differentiation and bone formation. Endocrinology 146:1226–1235
55. **Lazarenko OP, Rzonca SO, Hogue WR, Swain FL, Suva LJ, Lecka-Czernik B** 2007 Rosiglitazone induces decreases in bone mass and strength that are reminiscent of aged bone. Endocrinology 148:2669–2680
56. **Paulik MA, Lenhard JM** 1997 Thiazolidinediones inhibit alkaline phosphatase activity while increasing expression of uncoupling protein, deiodinase, and increasing mitochondrial mass in C3H10T1/2 cells. Cell Tissue Res 290:79–87
57. **Rzonca SO, Suva LJ, Gaddy D, Montague DC, Lecka-Czernik B** 2004 Bone is a target for the antidiabetic compound rosiglitazone. Endocrinology 145:401–406
58. **Sottile V, Seuwen K, Kneissel M** 2004 Enhanced marrow adipogenesis and bone resorption in estrogen-deprived rats treated with the PPARγ agonist BRL49653 (rosiglitazone). Calcif Tissue Int 75:329–337
59. **Grey A, Bolland M, Gamble G, Wattie D, Horne A, Davidson J, Reid IR** 2007 The peroxisome proliferator-activated receptor-γ agonist rosiglitazone decreases bone formation and bone mineral density in healthy postmenopausal women: a randomized, controlled trial. J Clin Endocrinol Metab 92:1305–1310
60. **Hampton T** 2007 Diabetes drugs tied to fractures in women. JAMA 297:1645
61. **Meymeh RH, Wooltorton E** 2007 Diabetes drug pioglitazone (Actos): risk of fracture. Can Med Assoc J 177:723–724
62. **Wan Y, Chong LW, Evans RM** 2007 PPAR-γ regulates osteoclastogenesis in mice. Nat Med 13:1496–1503
63. **Shoelson SE, Herrero L, Naaz A** 2007 Obesity, inflammation, and insulin resistance. Gastroenterology 132:2169–2180
64. **Stienstra R, Duval C, Keshtkar S, van der Laak J, Kersten S, Müller M** 2008 PPARγ activation promotes infiltration of alternatively activated macrophages into adipose tissue. J Biol Chem 283:22620–22627
65. **Welch JS, Ricote M, Akiyama TE, Gonzalez FJ, Glass CK** 2003 PPARγ and PPARδ negatively regulate specific subsets of lipopolysaccharide and IFN-γ target genes in macrophages. Proc Natl Acad Sci USA 100:6712–6717
66. **Katayama K, Wada K, Miyoshi H, Ohashi K, Tachibana M, Furuki R, Mizuguchi H, Hayakawa T, Nakajima A, Kadowaki T, Tsutsumi Y, Nakagawa S, Kamisaki Y, Mayumi T** 2004 RNA interfering approach for clarifying the PPARγ pathway using lentiviral vector expressing short hairpin RNA. FEBS Lett 560:178–182